

# Synergistic Supramolecular Encapsulation of Amphiphilic Hyperbranched Polymer to Dyes

Cuihua Liu, Chao Gao,\* and Deyue Yan

College of Chemistry and Chemical Engineering, Shanghai Jiao Tong University,  
800 Dongchuan Road, Shanghai 200240, P. R. China

Received April 10, 2006; Revised Manuscript Received September 8, 2006

**ABSTRACT:** A novel synergistic effect during supramolecular host–guest encapsulations of core–shell amphiphilic hyperbranched polymers to two kinds of dyes was reported. Two kinds of palmityl chloride-modified hyperbranched polymer, polyamidoamine (HPAMAM10K-C16) and poly(sulfone–amine) (HPSA11K-C16), were used as the hosts of supramolecular encapsulations, and water-soluble dyes such as methyl orange (MO) and methyl blue (MB) were selected as the corresponding guests. In cases of single-dye encapsulations, each host can extract one kind of guest from water phase into chloroform phase with a certain loading capacity ( $C_{\text{load}}$ ). In the double-dye encapsulations, a pair of dyes, MO and MB, was employed as the guests. The  $C_{\text{load}}$  increased significantly for one or both of the pair dyes with the  $C_{\text{load}}$  of the single-dye encapsulation as the reference. This is defined as synergistic encapsulation in this paper. For the HPAMAM10K-C16,  $C_{\text{load}}$  of MO can be increased by about 100% with the cooperation of MB. For HPSA11K-C16,  $C_{\text{load}}$  of MB can be raised to a 40–100-fold level of single-dye encapsulation without loss of MO. Experiments with different encapsulating sequence showed that the synergistic encapsulation for HPAMAM10K-C16 is a parallel-type process because the sequence has no significant impact on the  $C_{\text{load}}$  of each dye, while the case of HPSA11K-C16 is a cascade-type process since the results with different encapsulating order were different. The synergistic encapsulation phenomenon was confirmed by the measurements of  $^1\text{H}$  NMR, DSC, and TGA on the resulting dye-encapsulated hyperbranched polymers. In addition, investigations on the guest–host supramolecular systems with different pH indicated that the pH value has certain influence on the synergistic encapsulation  $C_{\text{load}}$ , but it was not the dominating factor for the synergistic encapsulation. The synergistic effect was found simultaneously in the supramolecular encapsulation of two hosts, indicating this effect is not limited to a peculiar dendritic polymer. The phenomenon presented here will trigger further application of dendritic and other complex polymeric materials in the supramolecular host–guest chemistry.

## Introduction

The history of host–guest supramolecular chemistry of dendritic polymers can be dated to the early of 1980s, when Maciejewski<sup>1</sup> proposed the possibility for trapping guest molecules inside hosts of dendritic macromolecules. Triggered by the work of encapsulating dyes into dendritic box, research efforts in this area have grown rapidly.<sup>2–5</sup> Some research groups were interested in the synthesis and characterization of dendrimer-encapsulated metal nanoparticles<sup>6</sup> and their uses as catalysts.<sup>7</sup> Some others gave their attention to the core–shell amphiphilic dendritic polymers and achieved good results. These mainly included the synthesis of amphiphilic dendritic polymers with a hydrophobic core surrounded by a hydrophilic shell and their application in delivering hydrophobic compounds<sup>8–10</sup> and the synthesis of amphiphilic dendritic polymers with a hydrophilic core surrounded by a hydrophobic shell<sup>11</sup> and their application in transferring water-soluble dyes,<sup>11–15</sup> such as rose bengal, congo red, eosin Y, fluorescein, bromophenol blue, methyl red, and methyl orange, from an aqueous solution to an apolar solvent. During the transferring process, the polymeric macromolecules encapsulated the small dye molecules, forming host–guest supramolecules. In this regard, most of the researches focused on the encapsulation behavior of dendrimers, especially the modified poly(amidoamine) (PAMAM)<sup>9,10,16</sup> and poly(propyleneimine) (PPI)<sup>12,17,18</sup> dendrimers.

Compared with dendrimers,<sup>19</sup> another important subclass of dendritic macromolecules, hyperbranched polymers, can be

prepared by a cost-effective methodology of one-step polymerization of  $\text{AB}_x$  ( $x \geq 2$ )-type monomers, without the numerous protection, deprotection, and purification steps during the preparation process.<sup>20</sup> Although their structure is not so perfect as that of dendrimers, hyperbranched polymers still have many similar characteristics and properties of dendrimers, such as three-dimensional globular architecture, numerous cavities, and plenty of peripheral functional groups, which offer hyperbranched polymers the possibility of promising usage in the topological encapsulation area. As early as in 1990, hyperbranched polyphenylene was ever used to encapsulate *p*-toluidine.<sup>3</sup> Some other hyperbranched polymers, mainly including hyperbranched polyglycerols,<sup>11</sup> polyesters,<sup>21</sup> and poly(ethyleneimine) (PEI),<sup>5,14</sup> also have been used to encapsulate guests. Frey and co-workers<sup>11</sup> encapsulated dyes into amphiphilic hyperbranched polyglycerols successfully and investigated the release condition of the encapsulated dyes. Haag et al.<sup>14</sup> synthesized a pH-responsive hyperbranched polymer and found it could selectively release the encapsulated guest molecules by adjusting pH. Recently, Frey et al.<sup>5</sup> reported that the quaternization of amino groups of functionalized hyperbranched PEI can improve the dye-loading capacity.

However, up to now, almost all of the dye encapsulation-related works reported were concentrated on the single-dye encapsulation in which only one kind of dye was used as the guest and encapsulated into dendritic boxes. A key question hence appears: is it possible to encapsulate more than one kind of dyes into the single-molecule level dendritic nanobox? We are very interested in the multidye encapsulation, in which multiple kinds of dyes are used as the guests, because it promises

\* Corresponding author: Tel (+86) 21-5474 2665; Fax (+86) 21-5474 1297; e-mail chaogao@sjtu.edu.cn.

extensive applications in the area of supramolecular science and nanotechnology. What will happen when an aqueous solution containing two or more kinds of dyes is mixed with an organic (e.g., chloroform) solution of an amphiphilic dendritic polymer? Two consequences are easily conceivable: (1) at least one kind of dye is selectively encapsulated into dendritic boxes, which can be defined as selective (multidye) encapsulation;<sup>5,13,14,17</sup> and (2) the dyes are encapsulated into dendritic boxes with a stochastic manner and the loading capability ( $C_{\text{load}}$ ) of each dye is lower than that of single-dye encapsulation, which is termed as stochastic or random (multidye) encapsulation. Except the two cases, we discovered the third one when methyl orange and methyl blue were selected as the pair of guests: the loaded amount of one dye increased significantly as compared with the case of single-dye encapsulation with the cooperation of another one. This novel phenomenon is coined as synergistic (multidye) encapsulation and discussed herein.

## Experimental Section

**Materials.** The palmityl chloride-functionalized amphiphilic hyperbranched poly(amidoamine) (named HPAMAM10K-C16,  $M_n = 10\,780$ , PDI = 2.39, ca. 61% amino groups were functionalized)<sup>22</sup> and poly(sulfone-amine) (named HPSA11K-C16,  $M_n = 11\,150$ , PDI = 1.67, ca. 65% amino groups were functionalized)<sup>23</sup> were synthesized in our lab according to the procedures published before. The hyperbranched poly(amidoamine) (HPAMAM) was synthesized by polycondensation of methyl acrylate (MA) and diethylenetriamine (DETA) (1.2/1 mole ratio)<sup>22</sup> (for synthesis details, see Supporting Information, SM1). The hyperbranched poly(sulfone-amine) (HPSA) was synthesized by polyaddition of divinyl sulfone and 1-(2-aminoethyl)piperazine (1/1 mole ratio).<sup>23</sup> The dye of methyl orange, 4-[4-(dimethylamino)phenylazo]benzenesulfonic acid sodium salt (MO), was purchased from Tianjin No.3 Chemical Reagent Factory. The dye of methyl blue, ((4-bis(*p*-(sulfoanilino)-phenyl)methylene-2,5-cyclohexadien-1-ylidene)amino)benzenesulfonic acid disodium salt (MB), and hydrochloric acid (HCl) were purchased from Sinopharm Chemical Reagent Co., Ltd. All of them were used as received. The water used to prepare the dye solution was deionized water after double distillations.

**Instrumentation.** UV/vis spectra were recorded on a Perkin-Elmer Lambda 20/2.0 UV/vis spectrometer.  $^1\text{H}$  NMR measurements were carried out on a Varian Mercuryplus 400 NMR spectrometer with  $\text{CDCl}_3$  as solvent. Dynamic light scattering (DLS) measurements were performed in chloroform solution at 25 °C by using Zetasizer Nano S (Malvern Instruments Ltd., Malvern, Worcestershire, UK) at a wavelength of 632 nm and a scattering angle of 173°. The concentrations of the polymer solutions were 0.05, 0.50, and 15 g/L. Prior to analysis, the solutions were filtered with disposable syringe filters of 0.45  $\mu\text{m}$  pore size. The pH values were measured by a RIDAO pH5-2C digital pH meter. Differential scanning calorimetric (DSC) measurements were conducted under nitrogen on a Perkin-Elmer Pyris-1 DSC thermal analyzer. Samples were heated from -60 to 100 °C for the first scan, then cooled to -60 °C, and then heated to 100 °C for the second scan. Thermogravimetric analysis (TGA) was performed under nitrogen on a Perkin-Elmer Pyris-7 thermal analyzer. All samples were heated at 20 °C/min heating rate.

**Single-Dye Encapsulation.** Typically, a 6 mL aqueous solution of MO or MB ( $1.0 \times 10^{-3}$  M) was mixed with a 6 mL chloroform solution of the amphiphilic hyperbranched polymer (HPAMAM10K-C16 or HPSA11K-C16, 0.05 g/L) in a glass bottle. The mixture was shaken by hand for 10 min to ensure the two phases were mixed adequately. The bottom layer of chloroform solution was transferred to a 1 cm UV/vis cuvette after the two phases separated completely, and its UV/vis spectrum was recorded. In all of the experiments, the dye in the aqueous solution was greatly excessive to ensure its encapsulated amount achieved the maximum of the loading capacity ( $C_{\text{load}}$ ). A series of MO (or MB) solutions with different pH were prepared by adding aqueous HCl to the original

solution and used in the experiments to investigate the pH influence on the corresponding  $C_{\text{load}}$ .

**One-Step Double-Dye Encapsulation.** Typically, a 6 mL aqueous solution containing  $1.0 \times 10^{-3}$  M MO and  $1.0 \times 10^{-3}$  M MB was mixed with an equal volume of polymer chloroform solution (0.05 g/L). The same protocol as that of the single-dye encapsulation was used to record the corresponding UV/vis spectra. Note: in order to collect samples with enough quantity to do some other measurements such as NMR, DSC, and TGA, high concentrations of both dyes ( $2.0 \times 10^{-3}$  M) and polymer (0.5 g/L) were used; the corresponding UV-vis spectra of the diluted solution are comparable with those of one-step double-dye encapsulation aforementioned at the same concentration.

**Gradual Double-Dye Encapsulation.** Typically, when MO (or MB) was encapsulated in the polymer chloroform solution with the manner of single-dye encapsulation and achieved its saturation value, the top water and bottom chloroform phases were kept in the bottle. The aqueous solution of MB (or MO) ( $4.0 \times 10^{-3}$  M) was gradually added into the bottle by several times with given volumes each time. After every addition, the same protocol as that of the single-dye encapsulation was used to record the corresponding UV/vis spectrum.

## Results and Discussion

**I. Selection of Hosts and Guests.** To investigate host-guest double-dye encapsulation of hyperbranched polymers, the host of hyperbranched polymer and the guest of pair dyes should be carefully chosen in advance. In our experiments, palmityl chloride functionalized poly(amidoamine) (HPAMAM10K-C16) and poly(sulfone-amine) (HPSA11K-C16) were used as the hosts to encapsulate the guests of a pair dye, MO and MB. Scheme 1 shows the structures of the polymers and the dyes selected. The pair dyes are picked out from the family of water-soluble and oil insoluble dyes according to the following principles: (1) the absorption peaks of the pair dyes between 350 and 700 nm do not overlap each other so that the absorption intensities can be detected by UV/vis individually when the pair dyes are in a solution; (2) the difference between the molar absorption coefficients of pair dyes is not too big (or in the same order of magnitude), so that the absorption peaks can be accurately measured when concentrations of dyes are comparable; and (3) the existence of one dye has no interference on absorbance of the other one. Besides, we also considered the complementary structural characteristics of pair dyes for the purpose of synergistic encapsulation: MO is a rodlike molecule, while MB is cone- or platelike one.

**II. Encapsulations of the HPAMAM10K-C16. Single-Dye and One-Step Double-Dye Encapsulations of the HPAMAM-10K-C16.** After selecting the hosts and the guests, we carried out the single-dye encapsulation experiments to determine the  $C_{\text{load}}$  of each dye in chloroform solution of amphiphilic hyperbranched polymers (HPs) from the UV/vis spectrum of the corresponding bottom chloroform layer quantitatively by assuming the same absorption coefficients for the dyes in the amphiphilic polymer chloroform solutions and in aqueous solutions.<sup>11</sup> The dye absorption coefficients were gained from the calibration curve of the dye in aqueous solution. Then the aqueous solution containing both MO and MB was mixed with the chloroform solution of the HPAMAM10K-C16 to measure  $C_{\text{load}}$ s of dyes in the double-dye encapsulation. Such a double-dye encapsulation is called as one-step (double-dye) encapsulation.

Figure 1 displays the UV/vis spectra of single- and double-dye encapsulations for HPAMAM10K-C16. According to the absorption peak of the dye in the single-dye encapsulation (spectra 1 and 2), the  $C_{\text{load}}$  of each dye for the HPAMAM10K-C16 was determined, as listed in Table 1. In spectrum 3, two





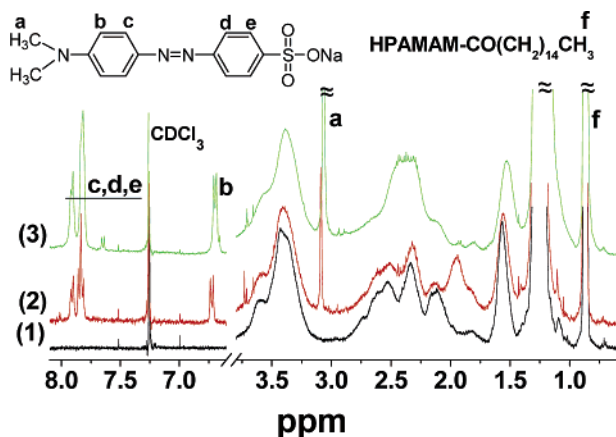


**Figure 2.**  $^1\text{H}$  NMR spectra of the neat HPAMAM10K-C16 (1), the MO-encapsulated HPAMAM10K-C16 (2), and the one-step double-dye encapsulated HPAMAM10K-C16 (3).

C16 at ca. 0.87 ppm ( $-\text{CH}_3$ , signal f) as the reference. The  $^1\text{H}$  NMR and UV/vis results are quite close, further implying that the UV/vis method to determine the  $C_{\text{load}}$  is still reliable in cases of double-dye encapsulation.

Generally, the substrates or guests can be encapsulated into a polytopic receptor or host via two manners: cascade- and parallel-type bindings.<sup>24</sup> In a cascade-type binding, different kinds of dyes are loaded into the host with a specific sequence and the encapsulating sequence has strong influence on  $C_{\text{load}}$ s accordingly, whereas such an influence is not significant in the parallel-type binding. Thus, we changed the dye-encapsulation sequence to probe the binding type in the double-dye encapsulation.

**Gradual Double-Dye Encapsulation of the HPAMAM10K-C16.** First, neat MO was encapsulated into the HPAMAM10K-C16 with a saturation value, followed by the gradual addition of the MB aqueous solution. The chloroform phase color gradually changed from orange-yellow to brown (Figure 3a), showing that MB molecules were trapped into the chloroform phase. The MO absorption increased gradually with increasing the added MB aqueous solution and approached to the maximum of ca. 1.132 (Figure 3b,c). This phenomenon reveals that MO molecules in the top water phase were further transferred into the chloroform phase with the cooperation of MB.

When the experiment was performed inversely, that is, adding MO to the saturated-encapsulation system of MB, the color of the chloroform phase gradually changed from blue to yellow-brown (Figure 4a). The MO absorption rapidly enhanced, exceeded the value of the single-dye encapsulation (0.536), increased to ca. 1.127, and then changed less with increasing the MO solution (Figure 4b,c). The MO molecules were also loaded into the HPAMAM10K-C16 with a much higher capacity by the aid of MB.

During the two gradual encapsulations, the MB absorption intensity vibrated near the value of its single-dye encapsulation (Figures 3b,c and 4b,c), and the maxima of MO absorption are almost equal to each other, proving that the double-dye encapsulation is a parallel-type process. The two maxima are a little higher than the maximum of one-step double-dye encapsulation (0.924), suggesting that the encapsulation is a dynamic process, and gradual encapsulation can favor the arrangement of supramolecular structure and topology, and the optimization of the interactions among MO, MB, and HPAMAM10K-C16, and thus improve the loading capacity to some extent.

**DSC Results.** When small molecules were loaded into the dendritic macromolecules, the thermal properties of the mac-

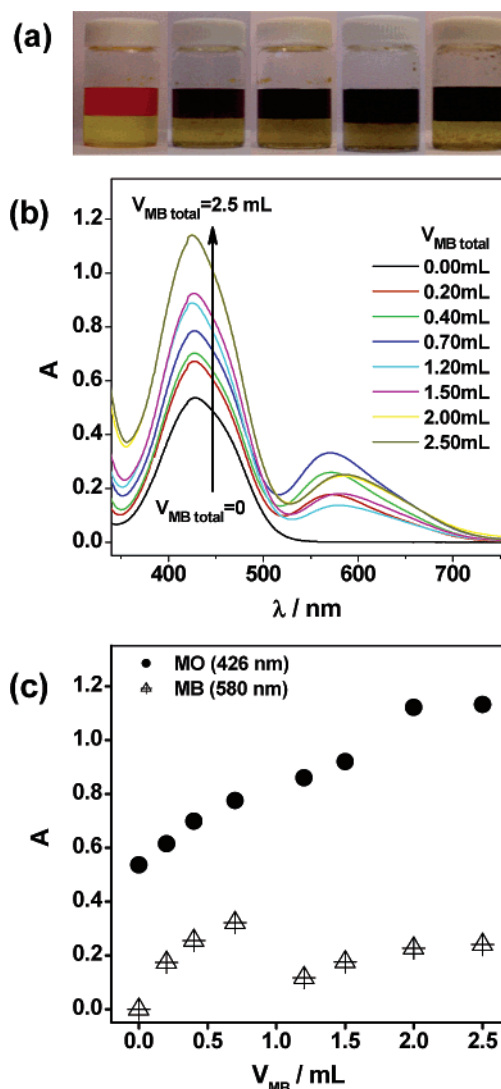


**Figure 3.** Selected results for the gradual double-dye encapsulation of the HPAMAM10K-C16 host by adding MB aqueous solution to the MO system. (a) Photographs (from left to right: total  $V_{\text{MB}}$  equals 0.0, 0.2, 0.4, 0.7, 1.2 mL). (b) UV/vis spectra of the HPAMAM10K-C16 chloroform solution with gradual adding MB aqueous solution to the MO system. (c) The corresponding absorbance values ( $A$ ) of MO at 426 nm and MB at 580 nm as a function of added volume of MB aqueous solution ( $V_{\text{MB}}$ ).

romolecules may be changed. This change can be possibly used to probe the existence of small molecules in the macromolecules in turn. Figure 5 shows the DSC curves of the neat HPAMAM10K-C16, MO-encapsulated HPAMAM10K-C16, double-dye encapsulated HPAMAM10K-C16, and the mixture of MO and HPAMAM10K-C16 (0.2:1 by mass, we name this sample "MO-mixed HPAMAM10K-C16"). From the heating stage of the DSC curves (Figure 5a), it can be found that the melting temperature range ( $\Delta T$ ) of HPAMAM10K-C16 is 13.35 °C (from 39.73 to 53.08 °C) for the neat HPAMAM10K-C16 and changes to 14.76 °C (from 36.05 to 50.81 °C) when it encapsulated MO molecules (for the sample of MO-encapsulated HPAMAM10K-C16) and even to 17.55 °C (from 30.63 to 48.18 °C) when it encapsulated both MO and MB molecules together (for the sample of double-dye encapsulated HPAMAM10K-C16). Accordingly, the melting point ( $T_m$ ) of HPAMAM10K-C16, the temperature value corresponding to the peak during the melting course, decreased from 48.05 to 45.37 °C when it encapsulated MO molecules and even to 41.65 °C when it encapsulated both MO and MB molecules together. From the

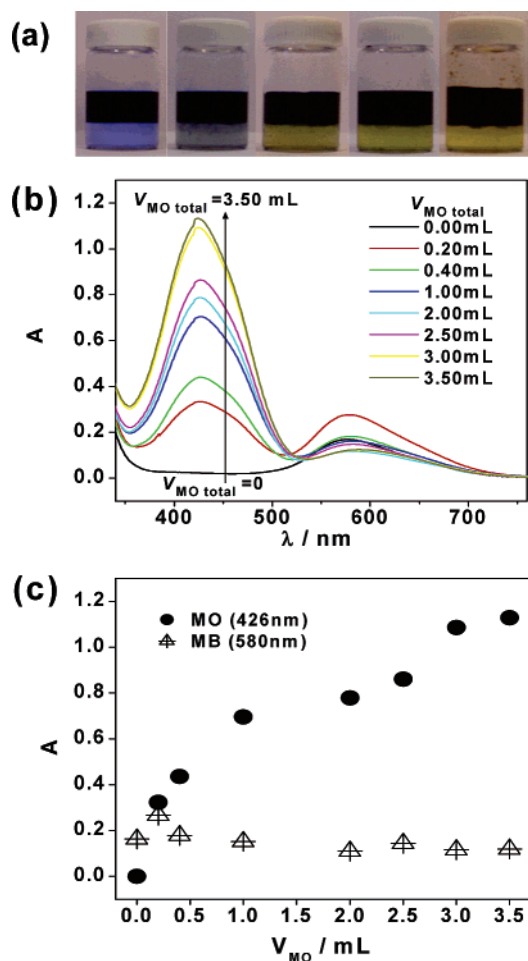


**Figure 4.** Selected results for the gradual double-dye encapsulation of the HPAMAM10K-C16 host by adding MO aqueous solution to the MB system. (a) Photographs (from left to right: total  $V_{\text{MO}}$  equals 0.0, 0.2, 0.4, 1.0, 2.0 mL). (b) UV/vis spectra of the HPAMAM10K-C16 chloroform solution with gradual adding MO aqueous solution to MB system. (c) The corresponding absorbance values ( $A$ ) of MO at 426 nm and MB at 580 nm as a function of added volume of MO aqueous solution ( $V_{\text{MO}}$ ).

cooling stage of the DSC curves (Figure 5b), it is also found that the crystallizing temperature range of HPAMAM10K-C16 turned wider (from 11.92 to 12.38 and 16.35 °C) and the crystallizing temperature ( $T_c$ ) decreased (from 41.21 to 39.24 and 36.2 °C) when the HPAMAM10K-C16 encapsulated MO or both MO and MB molecules. Such obvious differences of the melting or crystallizing temperature range and  $T_m$  or  $T_c$  for the samples of MO-encapsulated HPAMAM10K-C16 and double-dye encapsulated HPAMAM10K-C16 further confirm that much more dye molecules were transferred into the chloroform phase in the presence of another dye. This is in agreement with the results of UV/vis and  $^1\text{H}$  NMR measurements.

Another question appears: where were the transferred dye molecules localized? To probe that the small molecules were localized inside the HPAMAM10K-C16 macromolecules or just mixed with the macromolecules, we made the sample of the solid mixture of MO and HPAMAM10K-C16 (0.2:1 by mass) and also measured its DSC. The corresponding DSC curves of the MO-mixed HPAMAM10K-C16 are also shown in Figure 5. It is found that the  $T_m$  and  $T_c$  of the MO-mixed HPAMAM10K-C16 are about 48.08 °C and 41.61 °C, respectively. These values are almost same as those of the neat HPAMAM10K-C16 ( $T_m$  48.05 °C,  $T_c$  41.21 °C), whereas they are higher than

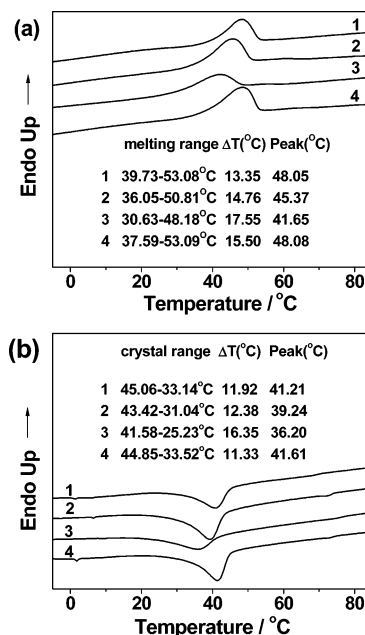


**Figure 5.** Heating stage (a) and cooling stage (b) of the DSC curves of the neat HPAMAM10K-C16 (1), the MO-encapsulated HPAMAM10K-C16 (2), the one-step double-dye encapsulated HPAMAM10K-C16 (3), and the MO-mixed HPAMAM10K-C16 (4). The heating or cooling rate was 20 °C/min.

those of the MO-encapsulated HPAMAM10K-C16 ( $T_m$  45.37 °C,  $T_c$  39.24 °C) and significantly higher than those of the double-dye encapsulated HPAMAM10K-C16 ( $T_m$  41.65 °C,  $T_c$  36.20 °C). The melting temperature range of the MO-mixed HPAMAM10K-C16 is 15.50 °C (from 37.59 to 53.09 °C), which is a little wider than that of the neat HPAMAM10K-C16, 13.35 °C. As is known, the existence of impurities with low molecular weight in a polymer matrix may broaden the melting temperature range and decrease the  $T_m$  or  $T_c$  of the polymer if the impurities interfere in the interactions between macromolecular chains. The comparable DSC results showed that the function of dye molecules in the samples of MO-encapsulated HPAMAM10K-C16 and double-dye encapsulated HPAMAM10K-C16 is different from that in the sample of MO-mixed HPAMAM10K-C16. Because of dye interaction with the polymer, the resulting supramolecular structures show different thermal properties compared with the neat polymer.

The decrease of the  $T_m$  and  $T_c$  and the widening of the melting and crystallizing temperature ranges for the samples of dye-encapsulated HPAMAM10K-C16 can be explained as follows. The volume of small molecules in the macromolecules makes the hydrophobic arms of HPAMAM10K-C16 packed more loosely and weakens the interactions between macromolecular chains. This is an evidence of the small molecules lying in the HPAMAM10K-C16 macromolecules. The difference between  $T_m$ s of the neat HPAMAM10K-C16 and that of double-dye encapsulated HPAMAM10K-C16 (6.4 °C) is greater than the difference between  $T_m$ s of the neat HPAMAM10K-C16 and one-dye encapsulated HPAMAM10K-C16 (2.68 °C) by about 138%, also proving that dye molecules were loaded into the HPAMAM10K-C16 macromolecules and indicating that the  $C_{\text{load}}$  of MO in the case of double-dye encapsulation was much higher than that of single-dye encapsulation. Considering the results obtained from UV/vis measurements, we can say that synergistic encapsulation did happen to the host of HPAMAM10K-C16.

**TGA Results.** Figure 6 shows the TGA weight loss curves of neat dyes, the neat HPAMAM10K-C16, the dye-encapsulated HPAMAM10K-C16, and the MO-mixed HPAMAM10K-C16.

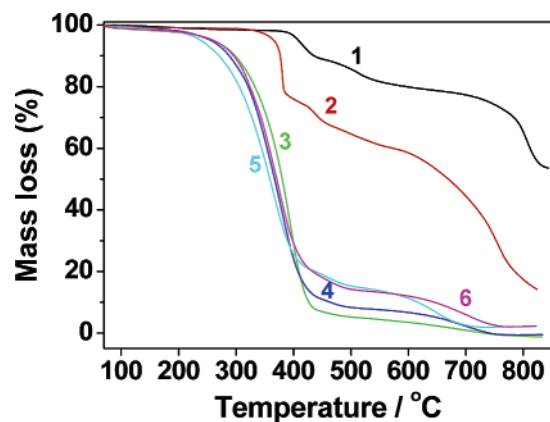


**Figure 6.** TGA weight loss curves of neat MB (1), neat MO (2), the neat HPAMAM10K-C16 (3), the MO-encapsulated HPAMAM10K-C16 (4), the one-step double-dye encapsulated HPAMAM10K-C16 (5), and the MO-mixed HPAMAM10K-C16 (6).

There are three obvious stages of weight loss for the neat MO: before 405 °C, 405–600 °C, and after 600 °C. Its total weight loss before 600 °C is ca. 41.489 wt %. For the MB, there are also three stages of weight loss: before 435 °C, 435–600 °C, and after 600 °C. Before 600 °C, the weight loss of MB is ca. 20.130 wt %. The weight loss of the MO-encapsulated HPAMAM10K-C16 before 600 °C (93.302 wt %) is lower than that of the neat HPAMAM10K-C16 (ca. 96.515 wt %), confirming the existence of MO in the product of MO-encapsulated HPAMAM10K-C16. Calculated from the data of the weight loss, the content of MO is ca. 0.0620 g/g of HPAMAM10K-C16. This value is lower than that obtained from the UV/vis spectra. It is likely attributed to the following reasons: (1) the error of the dye absorption coefficients between in the chloroform and in the water of calibration; (2) the error resulting from the TGA measurements. The weight loss of the double-dye encapsulated HPAMAM10K-C16 before 600 °C (88.738 wt %) is much lower than that of the MO-encapsulated HPAMAM10K-C16 (93.302 wt %), proving that the existence of both dyes or much more MO molecules were further loaded into the HPAMAM10K-C16.

In addition, because of the encapsulation of small molecules in the macromolecules, the interactions among the polymer arms were weakened, and then the HPAMAM10K-C16 showed lower  $T_m$  as compared with the neat HPAMAM10K-C16, as mentioned above. If the small molecules were localized inside the macromolecules, rather than intermolecules, not only the  $T_m$  but also the decomposition temperature ( $T_d$ ) of the dye-loaded HPAMAM10K-C16 would be decreased. Actually, the  $T_d$  of the MO-encapsulated HPAMAM10K-C16 (the temperature of 5% and 10% weight loss is ca. 256.8 and 288.8 °C, respectively) is obviously lower than that of the neat HPAMAM10K-C16 (the point of 5% and 10% weight loss is ca. 260.4 and 298.4 °C, respectively); the  $T_d$  of the double-dye encapsulated HPAMAM10K-C16 (the point of 5% and 10% weight loss is ca. 239.3 and 270.6 °C, respectively) is much lower than that of the MO-encapsulated HPAMAM10K-C16. By comparison, the  $T_d$  of the MO-mixed HPAMAM10K-C16 (the point of 5% and 10% weight loss is ca. 260.8 and 296.2 °C, respectively) is quite close to that of the neat HPAMAM10K-C16 but considerably higher than that of the MO-encapsulated HPAMAM10K-C16. These TGA results are in good accordance with the DSC ones, further confirming that (1) the MO molecules transferred into the chloroform phase were trapped into the HPAMAM10K-C16 macromolecules to form the host–guest supramolecules,

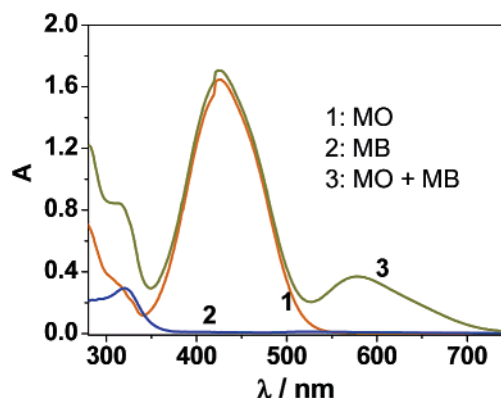


**Figure 7.** UV/vis spectra of the chloroform phase after the single- and one-step double-dye encapsulations of the HPSA11K-C16.

not just mixed with the macromolecules, and (2) synergistic encapsulation occurred in the double-dye encapsulation.

**DLS Measurements.** Moreover, dynamic light-scattering (DLS) measurements showed that no aggregation peak was found wherever the concentration of amphiphilic HPs in chloroform was low or high. The system is still a real solution even though the HP concentration is as high as 15 g/L. For the chloroform solutions of the MO-encapsulated HPAMAM10K-C16, the similar results to those of the neat HPAMAM10K-C16 were obtained in the DLS measurements, and no aggregation peak was observed either (see Supporting Information, SM2). The combinations of the DLS and other measurements verify that the transferred dyes were not localized at the space among the macromolecules or in assembled micelles, but inside the cavity of individual hyperbranched macromolecules.

**III. Encapsulations of the HPSA11K-C16. Double-Dye Encapsulation of the HPSA11K-C16.** To justify the generality of such a synergistic encapsulation, we employed another amphiphilic hyperbranched polymer, HPSA11K-C16, with much longer chain segments between neighboring units to perform the same double-dye encapsulations. The results are also collected in Table 1. Significantly, the  $C_{load}$  of MB was improved from little (ca. 0.05) ( $A_{MB} = 0.009$ ) to 2.04 ( $A_{MB} = 0.359$ ) d.m./M., without the decrease of MO, in the one-step double-dye encapsulation. The  $C_{load}$  of MB is increased by about 40-fold as compared with that of the single-dye encapsulation (see Table 1 and Figure 7). Compared with the HPAMAM10K-C16, HPSA11K-C16 exhibits much higher loading capabilities for both MO and MB in the synergistic double-dye encapsulation, which can be attributed to the bigger cavities of the HPSA11K-C16 resulted from its longer chain segments than those of the HPAMAM10K-C16.

Gradual double-dye encapsulations were also conducted for the host of HPSA11K-C16. When MO was added to the MB system (MB aqueous solution + MB-saturated HPSA11K-C16 chloroform solution), the color of the chloroform phase gradually changed from blue to deep-brown, indicating the double-dye encapsulation happened (Figure 8a). During this process, both MB and MO absorptions increased dramatically and then reached saturation values of ca. 0.389 and 1.669, respectively (Figure 8b,c), around which the absorptions fluctuated if more MO solution was added. Interestingly, both saturation values are quite close to corresponding values of the one-step double-dye encapsulation (therein,  $A_{MB} = 0.359$  and  $A_{MO} = 1.695$ ), implying that the efficiencies of the two double-dye encapsulation manners are almost equivalent. In fact, the two processes are comparable in essence because the quantity of the first



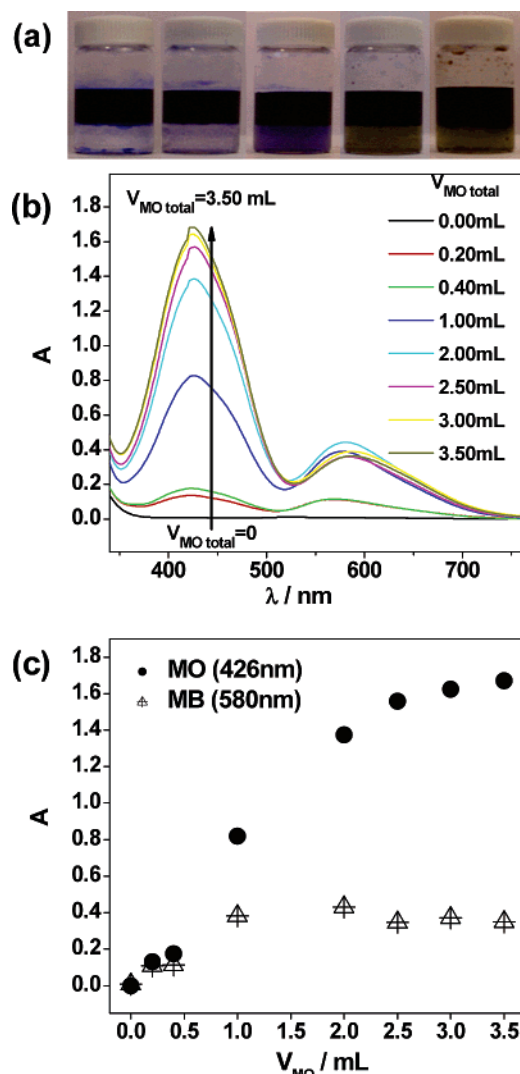


**Figure 8.** Selected results for the gradual double-dye encapsulation of the HPSA11K-C16 host by adding MO aqueous solution to the MB system. (a) Photographs (from left to right: total  $V_{\text{MO}}$  equals 0.0, 0.2, 0.4, 1.0, 2.0 mL). (b) UV/vis spectra of the HPSA11K-C16 chloroform solution with gradual adding the MO aqueous solution to the MB system. (c) The corresponding absorbance values ( $A$ ) of MO at 426 nm and MB at 580 nm as a function of added volume of MO aqueous solution ( $V_{\text{MO}}$ ).

encapsulated MB is very tiny or negligible in the gradual encapsulation.

In the inversed-sequence experiment, adding a MB solution to a MO system, a different result was obtained. The color of the chloroform phase gradually changed from orange-yellow to dark-brown (Figure 9a). The absorption of MB increased rapidly and then achieved a saturation value of ca. 0.869, with increasing the volume of the MB solution (Figure 9b,c). This value corresponds to ca. 96-fold of the capacity of the single-dye encapsulation and ca. 2.4-fold of one-step double-dye encapsulation. The  $C_{\text{load}}$  of MO also changed little during this process (Figure 9b,c). Therefore, with the cooperation of MO, the loading capability of MB is almost increased by 2 orders of magnitude. The  $C_{\text{load}}$  of MB can be raised to a much higher level if MO was first encapsulated into the HPSA11K-C16, indicating that the double-dye encapsulation for HPSA11K-C16 is a cascade or semicascade process.

**DSC and TGA Results.** Again, DSC and TGA measurements were conducted for the neat polymer, dye-encapsulated polymer, and the mixture of dye and polymer to probe the

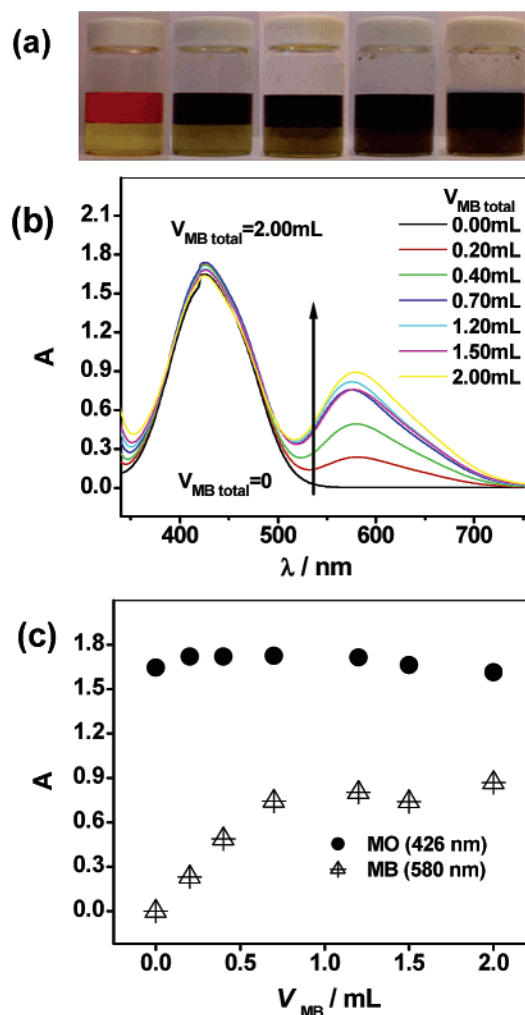


**Figure 9.** Selected results for the gradual double-dye encapsulation of the HPSA11K-C16 host by adding MB aqueous solution to the MO system. (a) Photographs (from left to right: total  $V_{\text{MB}}$  equals 0.0, 0.2, 0.4, 0.7, 1.2 mL). (b) UV/vis spectra of HPSA11K-C16 chloroform solution with gradual adding MB aqueous solution to MO system. (c) The corresponding absorbance values ( $A$ ) of MO at 426 nm and MB at 580 nm as a function of added volume of MB aqueous solution ( $V_{\text{MB}}$ ).

location of encapsulated dye molecules. Figure 10a shows the heating stage DSC curves of the samples. The melting temperature range ( $\Delta T$ ) of HPSA11K-C16 is 4.29 °C (from 38.76 to 43.05 °C) for the neat HPSA11K-C16 and changes to 8.69 °C (from 34.92 to 43.61 °C) when it encapsulated MO molecules for the sample of MO-encapsulated HPSA11K-C16 and to 9.84 °C (from 32.83 to 42.67 °C) when it encapsulated both MO and MB molecules together for the sample of double-dye encapsulated HPSA11K-C16. Consequently,  $T_m$  of HPSA11K-C16 decreased from 41.20 to 40.02 °C when it encapsulated MO molecules and to 36.63 °C when it encapsulated both MO and MB molecules together. While for the mixture of MO and HPSA11K-C16 (0.5:1 by mass, we name this sample "MO-mixed HPSA11K-C16"),  $T_m$  (41.12 °C) is very close to that of neat HPSA11K-C16 (41.20 °C), and its melting temperature range (4.38 °C) is also comparable with that of the neat HPSA11K-C16 (4.29 °C). Interestingly, the melting enthalpy ( $\Delta H$ ) of different sample is also distinct. The value of  $\Delta H$  decreases from 32.65 J/g for the neat HPSA11K-C16 to 4.90 J/g for the MO-encapsulated HPSA11K-C16 and to 2.73 J/g for the double-dye encapsulated HPSA11K-C16. However,  $\Delta H$  of the MO-mixed HPSA11K-C16 is 21.95 J/g, which is close to that of neat HPSA11K-C16 and much higher than those of

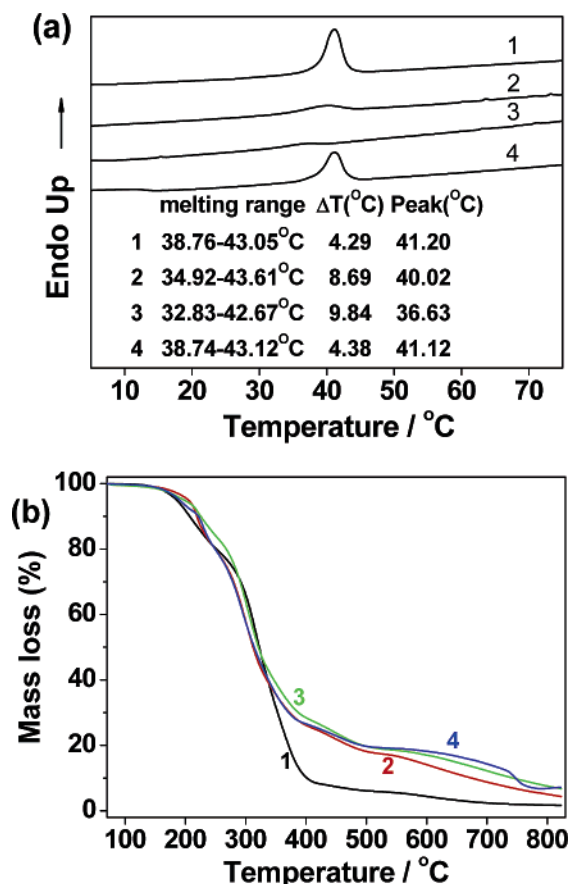


**Figure 10.** DSC curves (a) and TGA weight loss curves (b) of the neat HPSA11K-C16 (1), the MO-encapsulated HPSA11K-C16 (2), the one-step double-dye encapsulated HPSA11K-C16 (3), and the MO-mixed HPSA11K-C16 (4). The heating rate during the DSC measurements was 10  $^{\circ}\text{C}/\text{min}$ .

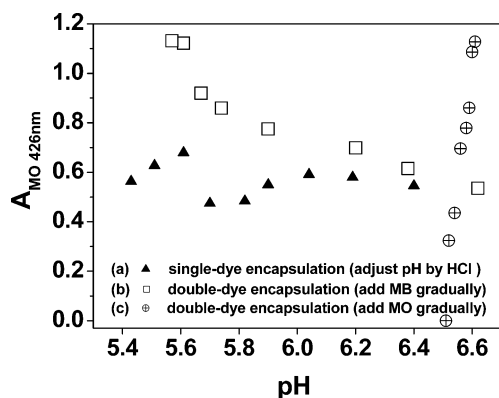
dye-encapsulated samples. Therefore, the DSC results further prove that the dye molecules located in different situation in the supramolecules from those in the MO-mixed HPSA11K-C16.

Figure 10b shows the TGA weight loss curves of the samples. The weight loss of the MO-encapsulated HPSA11K-C16 before 600  $^{\circ}\text{C}$  (85.903 wt %) is lower than that of the neat HPSA11K-C16 (ca. 95.593 wt %), confirming the existence of MO in the product of MO-encapsulated HPSA11K-C16. The weight loss of the double-dye encapsulated HPSA11K-C16 before 600  $^{\circ}\text{C}$  (82.989 wt %) is much lower than that of the MO-encapsulated HPSA11K-C16 (85.903 wt %), also proving that more dye molecules were loaded into the HPSA11K-C16.

From the DSC and TGA measurements, a similar conclusion to that of HPAMAM10K-C16 cases can be drawn: the dye molecules are located inside the cavity of individual macromolecules, and there is synergistic interaction between MO and MB molecules in the encapsulation behavior of HPSA11K-C16 indeed.

The outcomes described above enlighten us that (1) the synergistic encapsulation is not a particular but a general phenomenon and (2) the specific synergistic manners and results are dependent on many factors including structures and properties of hosts (polymers) and guests (dyes) and the interactions among them.

**IV. pH Influence on the Encapsulation.** Because the addition of another dye to the solution system of the first dye may change the pH of the solution, a question consequently appeared: whether the change of pH value has an effect on the



**Figure 11.** Relationship between the absorption of MO encapsulated by the HPAMAM10K-C16 in the bottom chloroform phase and pH value of the top aqueous solution. (a,  $\blacktriangle$ ) The absorption of MO encapsulated vs pH value of the neat MO aqueous solution ( $1.0 \times 10^{-3}$  M) adjusted by HCl in the single-dye encapsulation. (b,  $\square$ ) The absorption of MO encapsulated vs pH value of the MO-contained aqueous solution ( $1.0 \times 10^{-3}$  M) adjusted by adding the MB aqueous solution ( $4.0 \times 10^{-3}$  M) gradually in the double-dye encapsulation. (c,  $\oplus$ ) The absorption of MO encapsulated vs pH value of the MB-contained aqueous solution ( $1.0 \times 10^{-3}$  M) by adding MO aqueous solution ( $4.0 \times 10^{-3}$  M) gradually in the double-dye encapsulation.

double-dye encapsulation or not or whether the increment of  $C_{\text{load}}$  of one dye is caused by the pH variation of the solution in the presence of another dye. To answer this question, we investigated the influence of pH on the encapsulations. In the experiments of gradual double-dye encapsulation of HPAMAM10K-C16, the pH value of the system containing a 6.0 mL MO aqueous solution ( $1.0 \times 10^{-3}$  M) decreased from ca. 6.62 to ca. 5.52 when a 3.5 mL MB aqueous solution ( $4.0 \times 10^{-3}$  M) was added into the system gradually. In the same pH range (6.62–5.52), single-dye encapsulations of HPAMAM10K-C16 with different pH value were investigated. In the cases of MO, the absorbance of MO in the bottom chloroform phase changed a little, and the maximum is 0.68, when the pH of the top aqueous solution of MO changed from 6.62 to 5.52 (Figure 11a). By comparison, the maximum of absorbance of MO is about 1.132 in the case of gradual double-dye encapsulation aforementioned in the same pH range (6.62–5.52) (Figure 11b); this value (1.132) is much higher than the maximum resulted from the single-dye encapsulation experiments of pH variations (0.68). Therefore, the increment of the  $C_{\text{load}}$  (MO) in the double-dye encapsulations is not mainly due to the change of pH value during the course of adding another dye (MB) of the pair, but the existence of the other dye (MB).

When the 3.5 mL aqueous solution of MO ( $4.0 \times 10^{-3}$  M) was added gradually to the system containing a 6.0 mL aqueous solution of MB ( $1.0 \times 10^{-3}$  M) and 6.0 mL chloroform solution of HPAMAM10K-C16 (0.05 g/L), the pH of the top water phase increased from 6.51 to 6.61, and the absorbance of the chloroform phase increased gradually and reached a maximum of 1.127 (Figure 11c), as mentioned above. This maximum (1.127) is also much higher than that of single-dye encapsulations with different pH (0.68). This result also verified that the change of pH value is not the main reason for the augment of the  $C_{\text{load}}$ .

When the HPSA11K-C16 was chosen as the host, similar experiments of pH variation as the cases of HPAMAM10K-C16 aforementioned were also conducted. Figure 12a shows the absorbance of MB in the bottom chloroform phase at different pH values of the top aqueous solution in the single-dye encapsulation. It is found that the maximum absorbance of MB is about 0.071 in the pH range of 6.51 and 4.49. By



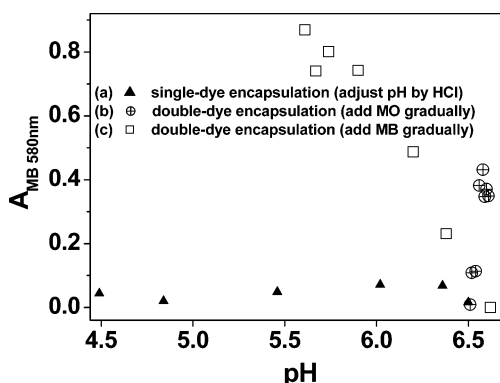


**Figure 12.** Relationship between the absorption of MB encapsulated by the HPSA11K-C16 in the bottom chloroform phase and pH value of the top aqueous solution. (a,  $\blacktriangle$ ) The absorption of MB encapsulated vs pH value of the neat MB aqueous solution ( $1.0 \times 10^{-3}$  M) adjusted by HCl in the single-dye encapsulation. (b,  $\oplus$ ) The absorption of MB encapsulated vs pH value of the MB-contained aqueous solution ( $1.0 \times 10^{-3}$  M) adjusted by adding MO aqueous solution ( $4.0 \times 10^{-3}$  M) gradually in the double-dye encapsulation. (c,  $\square$ ) The absorption of MB encapsulated vs pH value of the MO-contained aqueous solution ( $1.0 \times 10^{-3}$  M) by adding MB aqueous solution ( $4.0 \times 10^{-3}$  M) gradually in the double-dye encapsulation.

comparison, in the gradual double-dye encapsulation experiments (adding the aqueous solution of MO to the system of MB and HPSA11K-C16), the maximum absorbance of MB is about 0.431 in the pH range 6.51–6.61 in the presence of MO (Figure 12b). When adding the aqueous solution of MB ( $4.0 \times 10^{-3}$  M) gradually to the system containing the aqueous solution of MO ( $1.0 \times 10^{-3}$  M, 6.0 mL) and the chloroform solution of HPSA11K-C16 (0.05 g/L, 6.0 mL), the pH varied in the range 6.62–5.61, and the absorbance of MB increased gradually and reached about 0.869 (Figure 12c). Obviously, the absorbance maxima (0.431 and 0.869) of both gradual double-dye encapsulations are much higher than the maximum in the cases of single-dye encapsulations (0.071). Again, we can draw a conclusion that the significant increase of the  $C_{\text{load}}$  of MB in the double-dye encapsulations of HPSA11K-C16 is principally due to the existence and the cooperation of MO, and the contribution resulting from the pH variation to the increase of the  $C_{\text{load}}$  is neglectable in comparison with that of the synergistic effect.

## Conclusions

We discovered and investigated the synergistic encapsulation phenomenon of amphiphilic HPs in the process of double-dye host–guest encapsulation. With the cooperation of MB, the loading capacity of MO can be doubled for the HPAMAM10K-C16. For the HPSA11K-C16, the loading capacity of MB can be increased to a 96-fold level of single-dye encapsulation with almost no loss of MO. Through the manner of gradual encapsulation, the synergistic encapsulation type was probed. Parallel-type and cascade-type synergistic encapsulations were found respectively in the cases of HPAMAM10K-C16 and HPSA11K-C16. The synergistic encapsulation was confirmed by the combinations of UV/vis,  $^1\text{H}$  NMR, DSC, TGA, and DLS measurements. The synergistic encapsulation can be explained by the compatible functions of the sizes of dye molecules, the structures of dyes, the electrostatic acid–base interactions among the dyes and the polymer, the polymer structure, the sizes of cavities in the polymer, and the interactions between different dyes. We believe that this discovery will remarkably extend the ken of dendritic and other complex polymers applied in supramolecular science and technology, nanoengineering, and

medicine, enlighten us to dig out more new areas for macromolecules, and assemble or fabricate novel structures and devices by using such discoveries.

**Acknowledgment.** Financial support from the National Natural Science Foundation of China (Nos. 20304007, 50473010, 50233030), the Program for New Century Excellent Talents in University, the Foundation for the Author of National Excellent Doctoral Dissertation of China (No. 200527), Rising-Star Program Foundation of Shanghai (No. 03QB14028), and Fok Ying Tung Education Foundation (No. 91013) is greatly appreciated.

**Supporting Information Available:** Synthesis and characterization of HPAMAM10K-C16 (SM1) and DLS results of HPAMAM10K-C16 and MO-encapsulated HPAMAM10K-C16 (SM2). This material is available free of charge via the Internet at <http://pubs.acs.org>.

## References and Notes

- (1) Maciejewski, M. J. *Macromol. Sci., Chem.* **1982**, *A17*, 689.
- (2) (a) Diederich, F.; Dick, K.; Griebel, D. *J. Am. Chem. Soc.* **1986**, *108*, 2273. (b) Naylor, A. M.; Goddard III, W. A.; Kiefer, G. E.; Tomalia, D. A. *J. Am. Chem. Soc.* **1989**, *111*, 2339. (c) Shea, K. J.; Sasaki, D. Y. *J. Am. Chem. Soc.* **1989**, *111*, 3442. (d) Caminati, G.; Turro, N. J.; Tomalia, D. A. *J. Am. Chem. Soc.* **1990**, *112*, 8515. (e) Tamada, J. A.; Kertes, A. S.; King, C. J. *Ind. Eng. Chem. Res.* **1990**, *29*, 1319. (f) Newkome, G. R.; Moorefield, C. N.; Baker, G. R.; Saunders, M. J.; Grossman, S. H. *Angew. Chem., Int. Ed. Engl.* **1991**, *30*, 1178. (g) Hawker, C. J.; Wooley, K. L.; Frechet, J. M. J. *J. Am. Chem. Soc.* **1993**, *115*, 4375. (h) Frechet, J. M. J. *Science* **1994**, *263*, 1710. (i) Střiriba, S. E.; Kautz, H.; Frey, H. *J. Am. Chem. Soc.* **2002**, *124*, 9698. (j) Chen, Y.; Shen, Z.; Frey, H.; Perez-Prieto, J.; Střiriba, S. E. *Chem. Commun.* **2005**, 755.
- (3) Kim, Y. H.; Webster, O. W. *J. Am. Chem. Soc.* **1990**, *112*, 4592.
- (4) Kumar, K. R.; Brooks, D. E. *Macromol. Rapid Commun.* **2005**, *26*, 155.
- (5) Chen, Y.; Shen, Z.; Pastor-Perez, L.; Frey, H.; Střiriba, S. E. *Macromolecules* **2005**, *38*, 227.
- (6) (a) Chechik, V.; Crooks, R. M. *J. Am. Chem. Soc.* **2000**, *122*, 1243. (b) Crooks, R. M.; Lemon, B. I.; Sun, L.; Yeung, L. K.; Zhao, M. Q. *Top. Curr. Chem.* **2001**, *212*, 81. (c) Slaght, M. Q.; Střiriba, S. E.; Gebbink, R. J. M. K.; Kautz, H.; Frey, H.; van Koten, G. *Macromolecules* **2002**, *35*, 5734. (d) Bhattacharjee, R. R.; Chakraborty, M.; Mandal, T. K. *J. Nanosci. Nanotechnol.* **2003**, *3*, 487. (e) Chung, Y. M.; Rhee, H. K. *J. Colloid Interface Sci.* **2004**, *271*, 131.
- (7) (a) Lang, H. F.; May, R. A.; Iversen, B. L.; Chandler, B. D. *J. Am. Chem. Soc.* **2003**, *125*, 14832. (b) Li, Y.; El-Sayed, M. A. *J. Phys. Chem. B* **2001**, *105*, 8938. (c) Rahim, E. H.; Kamounah, F. S.; Frederiksen, J.; Christensen, J. B. *Nano Lett.* **2001**, *1*, 499.
- (8) (a) Liu, M. J.; Kono, K.; Frechet, J. M. J. *J. Controlled Release* **2000**, *65*, 121. (b) Morgan, M. T.; Carnahan, M. A.; Immoos, C. E.; Ribeiro, A. A.; Finkelstein, S.; Lee, S. J.; Grinstaff, M. W. *J. Am. Chem. Soc.* **2003**, *125*, 15485. (c) Liu, H. B.; Jiang, A.; Guo, J.; Uhrich, K. E. *J. Polym. Sci., Part A: Polym. Chem.* **1999**, *37*, 703. (d) Stone, D. L.; Smith, D. K. *Polyhedron* **2003**, *22*, 763.
- (9) Esfand, R.; Tomalia, D. A. *Drug Discov. Today* **2001**, *6*, 427.
- (10) Kojima, C.; Kono, K.; Maruyama, K.; Takagishi, T. *Bioconjugate Chem.* **2000**, *11*, 910.
- (11) Sunder, A.; Kramer, M.; Hanselmann, R.; Mulhaupt, R.; Frey, H. *Angew. Chem., Int. Ed.* **1999**, *38*, 3552.
- (12) Baars, M. W. P. L.; Kleppinger, R.; Koch, M. H. J.; Yeu, S. L.; Meijer, E. W. *Angew. Chem., Int. Ed.* **2000**, *39*, 1285.
- (13) Balzani, V.; Ceroni, P.; Gestermann, S.; Gorka, M.; Kauffmann, C.; Vogtle, F. *Tetrahedron* **2002**, *58*, 629.
- (14) Kramer, M.; Stumbe, J. F.; Turk, H.; Krause, S.; Komp, A.; Delineau, L.; Prokhorova, S.; Kautz, H.; Haag, R. *Angew. Chem., Int. Ed.* **2002**, *41*, 4252.
- (15) Jang, C. J.; Ryu, J. H.; Lee, J. D.; Sohn, D.; Lee, M. *Chem. Mater.* **2004**, *16*, 4226.
- (16) (a) Twyman, L. J.; Beezer, A. E.; Esfand, R.; Hardy, M. J.; Mitchell, J. C. *Tetrahedron Lett.* **1999**, *40*, 1743. (b) Beezer, A. E.; King, A. S. H.; Martin, I. K.; Mitchell, J. C.; Twyman, L. J.; Wain, C. F. *Tetrahedron* **2003**, *59*, 3873. (c) Kolhe, P.; Misra, E.; Kannan, R. M.; Kannan, S.; Lieh-Lai, M. *Int. J. Pharm.* **2003**, *259*, 143. (d) Santo, M.; Fox, M. A. *J. Phys. Org. Chem.* **1999**, *12*, 293.
- (17) Pittelkow, M.; Christensen, J. B.; Meijer, E. W. *J. Polym. Sci., Part A: Polym. Chem.* **2004**, *42*, 3792.

- (18) (a) Stephan, H.; Spies, H.; Johannsen, B.; Klein, L.; Vogtle, F. *Chem. Commun.* **1999**, 1875. (b) Jansen, J. F. G. A.; de Brabander-van den Berg, E. M. M.; Meijer, E. W. *Science* **1994**, 266, 1226. (c) Stevelmans, S.; van Hest, J. C. M.; Jansen, J. F. G. A.; van Boxtel, D. A. F. J.; de Brabander-van den Berg, E. M. M.; Meijer, E. W. *J. Am. Chem. Soc.* **1996**, 118, 7398.
- (19) (a) Buhleier, E.; Wehner, W.; Vogtle, F. *Synthesis* **1978**, 2, 155. (b) Tomalia, D. A.; Baker, H.; Dewald, J.; Hall, M.; Kallos, G.; Martin, S.; Roeck, J.; Ryder, J.; Smith, P. *Polym. J.* **1985**, 17, 117. (c) Tomalia, D. A.; Baker, H.; Dewald, J.; Hall, M.; Kallos, G.; Martin, S.; Roeck, J.; Ryder, J.; Smith, P. *Macromolecules* **1986**, 19, 2466. (d) Tomalia, D. A.; Naylor, A. M.; Goddard III, W. A. *Angew. Chem., Int. Ed. Engl.* **1990**, 29, 138. (e) Bosman, A. W.; Janssen, H. M.; Meijer, E. W. *Chem. Rev.* **1999**, 99, 1665. (f) Dykes, G. M. *J. Chem. Technol. Biotechnol.* **2001**, 76, 903. (g) Klajnert, B.; Bryszewska, M. *Acta Biochim. Pol.* **2001**, 48, 199. (h) Tomalia, D. A.; Frechet, J. M. J. *J. Polym. Sci., Part A: Polym. Chem.* **2002**, 40, 2719. (i) Frechet, J. M. J. *Proc. Natl. Acad. Sci. U.S.A.* **2002**, 99, 4782. (j) Frechet, J. M. J. *J. Polym. Sci., Part A: Polym. Chem.* **2003**, 41, 3713.
- (20) (a) Flory, P. J. *J. Am. Chem. Soc.* **1952**, 74, 2718. (b) Kim, Y. H.; Webster, O. W. *Macromolecules* **1992**, 25, 5561. (c) Hawker, C. J.; Lee, R.; Frechet, J. M. J. *J. Am. Chem. Soc.* **1991**, 113, 4583. (d) Turner, S. R.; Walter, F.; Voit, B. I.; Mourey, T. H. *Macromolecules* **1994**, 27, 1611. (e) Inoue, K. *Prog. Polym. Sci.* **2000**, 25, 453. (f) Uhrich, K. E.; Hawker, C. J.; Frechet, J. M. J.; Turner, S. R. *Macromolecules* **1992**, 25, 4583. (g) Gao, C.; Yan, D. *Prog. Polym. Sci.* **2004**, 29, 183. (h) Jikei, M.; Kakimoto, M. *Prog. Polym. Sci.* **2001**, 26, 1233. (i) Voit, B. *J. Polym. Sci., Part A: Polym. Chem.* **2005**, 43, 2679. (j) Voit, B. I. *C. R. Chim.* **2003**, 6, 821. (k) Voit, B. *J. Polym. Sci., Part A: Polym. Chem.* **2000**, 38, 2505. (l) Kim, Y. H. *J. Polym. Sci., Part A: Polym. Chem.* **1998**, 36, 1685. (m) Kim, Y. H.; Webster, O. *J. Macromol. Sci., Polym. Rev.* **2002**, C42, 55. (n) Mori, H.; Müller, A. H. E. *Top. Curr. Chem.* **2003**, 228, 1.
- (21) Santra, S.; Kumar, A. *Chem. Commun.* **2004**, 2126.
- (22) Liu, C. H.; Gao, C.; Yan, D. Y. *Chem. Res. Chin. Univ.* **2005**, 21, 345.
- (23) (a) Yan, D. Y.; Gao, C. *Macromolecules* **2000**, 33, 7693. (b) Gao, C.; Yan, D. Y.; Zhang, B.; Chen, W. *Langmuir* **2002**, 18, 3708.
- (24) Lehn, J. M. *Science* **1985**, 227, 849.

MA0608065